

Longitudinal and transverse meson correlators in the deconfined phase from the lattice

Gert Aarts*, Chris Allton^{1*}, Justin Foley[†], Simon Hands* and Seyong Kim**

**Department of Physics, Swansea University, Swansea SA2 8PP, United Kingdom*

[†]*Department of Physics, Carnegie Mellon University, Pittsburgh, PA 15213, USA*

***Department of Physics, Sejong University, Seoul 143-747, Korea*

Abstract. It has long been known that QCD undergoes a deconfining phase transition at high temperature. One of the consequent features of this new, quark-gluon phase is that hadrons become unbounded. In this talk meson correlation functions at non-zero momentum are studied in the deconfined phase using the Maximum Entropy Method.

Keywords: Quark Gluon Plasma, Lattice QCD

PACS: 11.10.Wx, 14.40.Lb, 11.15.Ha, 12.38.Gc, 12.38.Mh

INTRODUCTION

QCD is well-known to be a strongly interacting and confining theory under “normal” conditions. However, it has long been theorised that at large energy scales (in temperature, T , or baryonic chemical potential, μ) it undergoes a transition to a deconfined (quark-gluon plasma) phase. This has been experimentally observed at CERN [1] and at the RHIC experiment at Brookhaven [2]. The exact nature of this transition is undergoing intense theoretical and experimental investigation. In fact, even the general features of the QCD phase diagram are still being mapped out (see Fig.1). As an example of this uncertainty, the Particle Data Book [3] does not contain a single reference to the deconfined phase of QCD! Properties of QCD at $T = \mu = 0$ are measured experimentally and calculated theoretically often to accuracy at the percent level or below. The same is certainly not true of the deconfined phase, where properties typically have much larger ($\sim 20\%$) errors associated with them, if they are known at all.

Physics at $T = \mu = 0$ is characterised by quantities such as hadronic masses and transition matrix elements, whereas the relevant quantities in the deconfined phase correspond to those of plasma physics: pressure, entropy, susceptibilities, and response functions. Of particular interest in this work are transport coefficients.

From general arguments based on the asymptotically free nature of QCD, the naive expectation is that quarks and gluons would be virtually free in the deconfined phase. However, at RHIC, a (relatively) strongly interacting phase was found with “almost instantaneous” equilibration and a small ratio of viscosity, η , to entropy density, s (both signs of “strong” coupling). These are characteristics of a so-called “Perfect Fluid”.

¹ Speaker

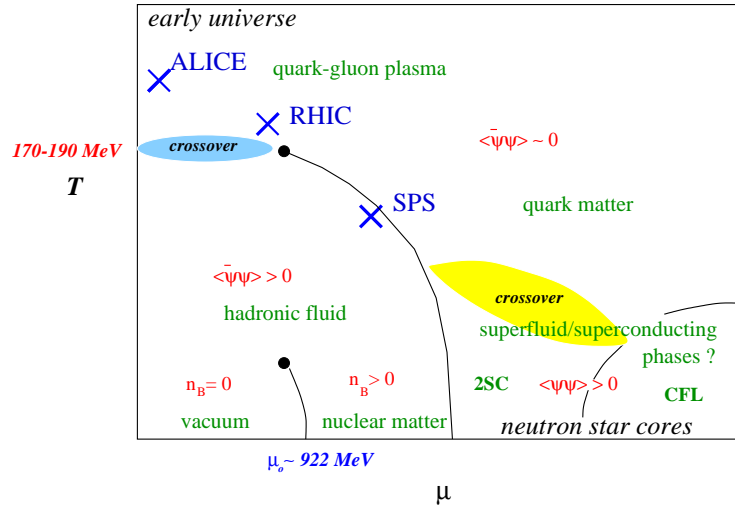


FIGURE 1. Illustrative phase diagram of QCD.

There is some theoretical basis for such small values of η/s in the plasma phase. A calculation relying on the correspondence between $\mathcal{N} = 4$ supersymmetric Yang-Mills theory and superstring theory in $AdS_5 \times S^5$ space-time predicts a lower bound for η/s [4, 5],

$$\eta/s \geq \frac{1}{4\pi} \quad \text{for } N_c, g^2 N_c \rightarrow \infty. \quad (1)$$

While this theory is not QCD, it gives a scale for this ratio in a strongly interacting theory [5].

Transport coefficients are essential properties of the plasma phase and can be derived theoretically from current-current spectral functions. We list some of them here.

Shear viscosity, η , which is obtained from off-diagonal energy-momentum correlators in the zero energy limit [6].

Bulk viscosity, ξ , which is obtained from diagonal energy-momentum correlators in the zero energy limit [7].

Electrical conductivity, σ , and **Diffusivity**, D , which are obtained from the energy dependence of vector meson spectral functions [8].

The aim of this talk is to make progress in the understanding of the deconfining mechanism by analysing mesonic systems simulated by a lattice calculation at $T \neq 0$ (but with $\mu = 0$). Naively, it is expected that the two (valence) quarks in these mesons should become unbound at the deconfining temperature, T_c . In practice this appears true for light quark states only, and charmonium states appear to remain bound until temperatures higher than T_c [9, 10]. Specifically we aim to determine the diffusivity through a lattice simulation of correlation functions of vector currents at non-zero momentum. This work extends our previous studies at zero momentum [8] where we calculated the electrical conductivity. A full version of this work is in preparation [11].

LATTICE BACKGROUND

The conventional approach to studying hadronic quantities with the lattice technique is via the imaginary-time dependence of Euclidean correlation functions of operators with well-defined quantum numbers. In the confined phase, each bound state (in the tower of states with those quantum numbers) contributes $\sim e^{-E_i t}$ to the correlation function, $G(t)$, where E_i is the state's energy. At large times, t , the lowest state dominates, so fitting $G(t)$ to an exponential form can trivially (in theory) determine E_0 .

In the deconfined phase, the situation is more subtle. Unbound states no longer contribute pure exponential terms to $G(t)$, and it is more appropriate to introduce the spectral function, $\rho(\omega, \vec{p})$,

$$G(t, \vec{p}) = \int_0^\infty \rho(\omega, \vec{p}) K(t, \omega) \frac{d\omega}{2\pi}, \quad (2)$$

where the (lattice) kernel is defined

$$K(t, \omega) = \frac{\cosh[\omega(t - 1/(2T))]}{\sinh[\omega/(2T)]}, \quad (3)$$

and we have allowed for a momentum dependence in the correlation function G and therefore in ρ . As usual, the temperature, T is the inverse temporal length, $1/(aN_t)$.

In the confined case, each non-decaying state i contributes a delta function, $\delta(\omega - E_i)$, to $\rho(\omega)$. A decaying state would have a spectral feature of finite width, and an unbound state would correspond to a continuous spectrum. By studying the temperature dependence of spectral functions the transition from the bound to deconfined phases can be observed.

As well as containing information on the stability or otherwise of hadronic states, $\rho(\omega, \vec{p})$ also can be used to extract transport coefficients (as described in Sec.1) and hydrodynamic structure.

However, despite the importance of the spectral function, and its simple definition in terms of the correlation function in eq.(2), it is notoriously difficult to extract. This is because it is an example of an ill-posed problem: there are (in general) more ω data points in $\rho(\omega)$ than there are t data points in the correlation function $G(t)$. The method which has now become fairly standard to overcome this problem is the *Maximum Entropy Method* (MEM) which is based on Bayesian statistics (for a review, see [12]). MEM is a very standard technique in fields which require image reconstruction/deconvolution, such as astronomy, crystallography, and the analysis of atomic/molecular spectra.

This work is an extension to our earlier work [8, 13, 14] to non-zero momentum. Specifically, we apply MEM to calculate $\rho(\omega, \vec{p})$ for mesonic correlation functions on lattice data with parameters summarised in Table 1. We used the quenched approximation with the standard Wilson gluonic and staggered fermionic actions, full details are given in [8]. Twisted boundary conditions [15, 16] were used to allow a finer resolution in momentum space for $G(t, \vec{p})$ (and therefore $\rho(\omega, \vec{p})$). In all 21 different momenta combinations were studied (ranging up to $|\vec{p}| \sim 10/L$) of which 17 are non-degenerate.

We follow our earlier work [8] where a singularity in $K(\omega, t)$ as $\omega \rightarrow 0$ was corrected by a simple redefinition of $K \rightarrow \omega K/(2T)$. This allows us to obtain reliable $\rho(\omega, \vec{p})$ estimates, even in the $\omega \rightarrow 0$ limit.

TABLE 1. Lattice parameters used in the simulation.

		Cold	Hot
Spatial Volume	$N_s^3 \times N_t$	$48^3 \times 24$	$64^3 \times 24$
Lattice spacings	a^{-1}	~ 4 GeV	~ 10 GeV
T	$1/(aN_t)$	$T \sim 160\text{MeV} \sim 0.62T_c$	$T \sim 420\text{MeV} \sim 1.5T_c$
Statistics	N_{cfg}	~ 100	~ 100

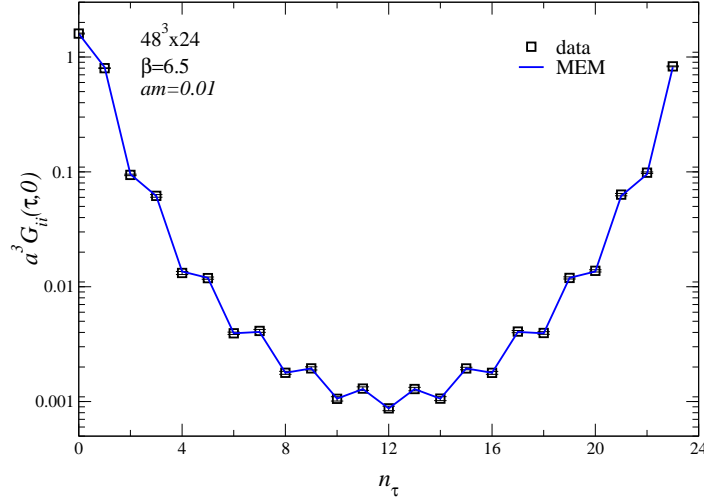


FIGURE 2. An example of the staggered correlation function showing the MEM analysis.

RESULTS

Our fermionic action uses staggered quarks so therefore the hadronic correlators are a mixture of states with opposite parity, see Fig.2. These can be decomposed into the following spectral representation,

$$G(t, \vec{p}) = \int_0^\infty \frac{d\omega}{2\pi} K(t, \omega) [\rho(\omega, \vec{p}) - (-1)^t \bar{\rho}(\omega, \vec{p})]. \quad (4)$$

This means that to recover the physical spectral function, the even and odd timeslices must be treated separately and then combined,

$$\rho = \frac{1}{2} (\rho^{\text{even}} + \rho^{\text{odd}}). \quad (5)$$

Since there are only $N_t = 24$ time slices in our lattices, the MEM analysis of the even and odd timeslices includes six timeslices (allowing for time reversal symmetry). This motivates the use of anisotropic lattices in future studies [9].

The electrical conductivity, defined

$$\frac{\sigma}{T} = \lim_{\omega \rightarrow 0} \frac{\rho_{ii}(\omega)}{6\omega T}, \quad (6)$$

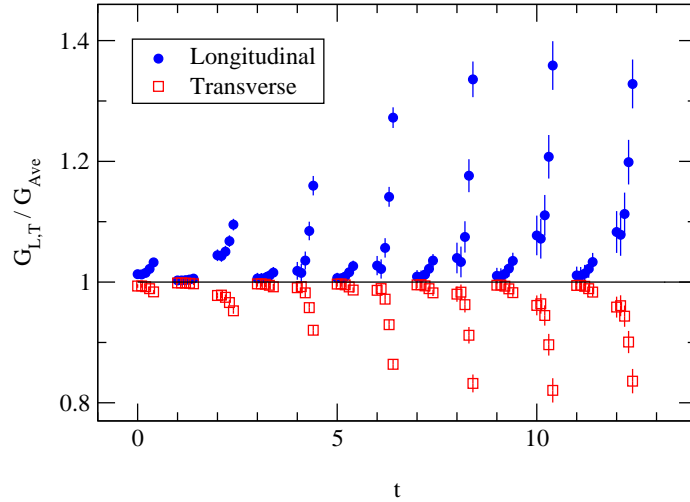


FIGURE 3. Longitudinal and transverse vector correlation functions normalised by the average correlation function, $G_{\text{Ave}} = G_{\text{L}} + 2G_{\text{T}}$, for various momenta, \vec{p} , as a function of time. Data points for each momenta (for a given time) are offset horizontally for clarity; from left to right they are $|\vec{p}|L = 0, 2, \pi, 2\pi, 3\pi$.

was found using this method [8], where ρ_{ii} is the spectral function for the spatial component of the vector correlator. The work presented here extends [8] by including non-zero momenta. In Fig.3, we plot the longitudinal and transverse vector correlation function versus time for various momenta. As can be seen, there is a distinct difference between the longitudinal and transverse correlators and a clear systematic effect as the momenta increase.

The diffusivity, D , can be obtained, in principle, from the momentum dependency of the longitudinal vector spectral function in the light quark mass limit (see e.g. [17]). In Fig. 4, the spectral functions for the longitudinal vector case are shown for both the $ma = 0.01$ and 0.05 quark masses. As can be seen, there is a clear non-zero intercept in the case of the 0.01 mass which is absent in the 0.05 case. It is this non-zero intercept in the 0.01 case which led us to determine the conductivity in [8]. Our future plans are to study this momentum dependency with the aim of independently determining D [11].

ACKNOWLEDGMENTS

CRA would like to thank the organiser of the workshop ‘‘Achievements and New Directions in Subatomic Physics’’. S.K. was supported by the National Research Foundation of Korea grant funded by the Korea government (MEST) No. 2009-0074027. We also acknowledge the STFC grant ST/G000506/1.

REFERENCES

1. U. W. Heinz and M. Jacob, [arXiv:nucl-th/0002042].

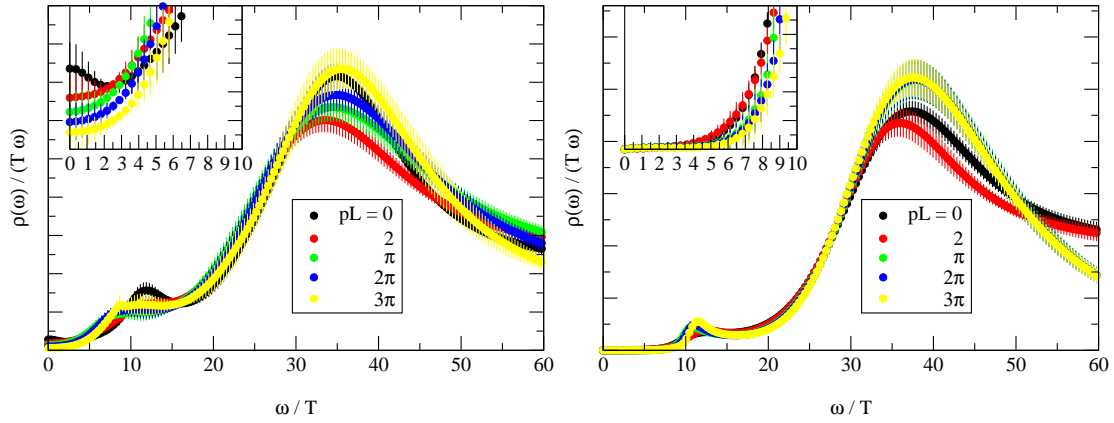


FIGURE 4. Longitudinal vector spectral function for various momenta in the hot case for $ma = 0.01$ [left], and $ma = 0.05$ [right].

2. I. Arsene *et al.* [BRAHMS Collaboration], Nucl. Phys. A **757** (2005) 1 [arXiv:nucl-ex/0410020]; B. B. Back *et al.*, Nucl. Phys. A **757** (2005) 28 [arXiv:nucl-ex/0410022]; J. Adams *et al.* [STAR Collaboration], Nucl. Phys. A **757** (2005) 102 [arXiv:nucl-ex/0501009]; K. Adcox *et al.* [PHENIX Collaboration], Nucl. Phys. A **757** (2005) 184 [arXiv:nucl-ex/0410003].
3. C. Amsler *et al.* [Particle Data Group], Phys. Lett. B **667**, 1 (2008).
4. G. Policastro, D. T. Son and A. O. Starinets, Phys. Rev. Lett. **87** (2001) 081601 [arXiv:hep-th/0104066].
5. P. Kovtun, D. T. Son and A. O. Starinets, Phys. Rev. Lett. **94** (2005) 111601 [arXiv:hep-th/0405231].
6. H. B. Meyer, Phys. Rev. D **76** (2007) 101701 [arXiv:0704.1801 [hep-lat]].
7. H. B. Meyer, Phys. Rev. Lett. **100** (2008) 162001 [arXiv:0710.3717 [hep-lat]].
8. G. Aarts, C. Allton, J. Foley, S. Hands and S. Kim, Phys. Rev. Lett. **99** (2007) 022002 [arXiv:hep-lat/0703008].
9. G. Aarts, C. Allton, M. B. Oktay, M. Peardon and J. I. Skullerud, Phys. Rev. D **76** (2007) 094513 [arXiv:0705.2198 [hep-lat]].
10. M. Asakawa and T. Hatsuda, Phys.Rev.Lett. **92**, 012001 (2004), [hep-lat/0308034]; S. Datta, F. Karsch, P. Petreczky and I. Wetzorke, Phys.Rev. **D69**, 094507 (2004), [hep-lat/0312037]; A. Jakovac, P. Petreczky, K. Petrov and A. Velytsky, Phys.Rev. **D75**, 014506 (2007), [hep-lat/0611017].
11. G. Aarts, C. Allton, J. Foley, S. Hands and S. Kim, *in preparation*.
12. M. Asakawa, T. Hatsuda and Y. Nakahara, Prog. Part. Nucl. Phys. **46**, 459(2001).
13. G. Aarts, C. Allton, J. Foley, S. Hands and S. Kim, PoS **LAT2006** (2006) 134 [arXiv:hep-lat/0610061].
14. G. Aarts, C. Allton, J. Foley, S. Hands and S. Kim, Nucl. Phys. A **785** (2007) 202 [arXiv:hep-lat/0607012].
15. P. F. Bedaque, Phys. Lett. B **593** (2004) 82 [arXiv:nucl-th/0402051].
16. J. M. Flynn, A. Juttner and C. T. Sachrajda [UKQCD Collaboration], Phys. Lett. B **632** (2006) 313 [arXiv:hep-lat/0506016].
17. Juhee Hong, Derek Teaney, [arXiv:1003.0699v1 [nucl-th]].